arXiv:cond-mat/0206200v1 [cond-mat.str-el] 12 Jun 2002

Convergence of energy-dependent incommensurate antiferromagnetic neutron scattering peaks to commensurate resonance in underdoped bilayer cuprates

Shiping Feng and Feng Yuan

Department of Physics, Beijing Normal University, Beijing 100875, China

National Laboratory of Superconductivity, Academia Sinica, Beijing 100080, China

Zhao-Bin Su

Institute of Theoretical Physics and Interdisciplinary Center of Theoretical Studies, Chinese Academy of Sciences, Beijing 100080, China

Lu Yu

The Abdus Salam International Centre for Theoretical Physics, 34014 Trieste, Itlay

Institute of Theoretical Physics and Interdisciplinary Center of Theoretical Studies, Chinese Academy of Sciences, Beijing 100080, China

Abstract

The recently discovered coexistence of incommensurate antiferromagnetic neutron scattering peaks and commensurate resonance in underdoped $YBa_2Cu_3O_{6+x}$ is calling for an explanation. Within the t-J model, the doping and energy dependence of the spin dynamics of the underdoped bilayer cuprates in the normal state is studied based on the fermion-spin theory by considering the bilayer interactions. Incommensurate peaks are found at $[(1 \pm \delta)\pi, \pi]$ and $[\pi, (1 \pm \delta)\pi]$ at low energies with δ initially increasing with doping at low dopings and then saturating at higher dopings. These incommensurate peaks are suppressed, and the parameter δ is reduced with

increasing energy. Eventually it converges to the $[\pi, \pi]$ resonance peak. Thus the recently observed coexistence is interpreted in terms of bilayer interactions.

74.25.Ha, 74.20.Mn, 74.72.Dn

Typeset using REVTEX

The interplay between antiferromagnetism (AF) and superconductivity (SC) in high T_c cuprates is well-established by now, [1] but its full understanding is still a challenging issue. Experimentally the inelastic neutron scattering (INS) can provide rather detailed information on the spin dynamics of doped single layer and bilayer cuprates. [2–10] An important issue is whether the behavior of AF fluctuations in these compounds is universal or not. A distinct feature of single layer $La_{2-x}Sr_xCuO_4$ (LSCO) is the presence of incommensurate antiferromagnetic (ICAF) peaks at low energy INS, *i.e.,* the AF scattering peaks are shifted from the AF wave vector [π,π] to four points [$\pi(1\pm\delta),\pi$] and [$\pi,(1\pm\delta)\pi$] (in units of inverse lattice constant) with δ as the incommensurability (IC) parameter, which depends on doping concentration, but not on energy. Moreover, ICAF is observed both above and below T_c in the entire range of doping, from underdoped to overdoped samples. [1–3] In contrast, a sharp resonance peak (around 41 meV) is observed in optimally doped bilayer $YBa_2Cu_3O_{6+x}$ (YBCO) at the commensurate AF wave vector [π,π] in the SC state. [4,5] Such a resonance has also been observed in underdoped YBCO samples with resonance energy scaling down with the SC T_c, being present both below and above T_c. [6] Recently, this resonance peak has been observed in another class of bilayer SC cuprates $Bi_2Sr_2CaCu_2O_{8+\delta}$ (BSCO). [7] Such a peak has, however, never been observed in LSCO. A very important new development is the observation of ICAF in underdoped YBCO in both SC and normal states, with INS pattern and doping dependence being very similar (linear in doping for low dopings) to that of LSCO. [8,9] However, the IC peak position is energy dependent in underdoped YBCO. A challenging issue for theory is to explain the coexistence of this energy-dependent ICAF scattering and commensurate resonance in bilayer cuprates.

Theoretically the ICAF has been interpreted, among others, in terms of Fermi surface nesting [11,12] or stripe formation. [13] The energy dependence of IC parameter δ on energy for underdoped YBCO makes the stripe interpretation rather difficult to accept. On the other hand, the commensurate resonance peak has been interpreted as due to spin-1 collective (particle-hole) excitations, [12,14,15] or particle-particle excitations, [16] or interlayer tunneling. [17] These theoretical treatments are mostly addressing the SC state, and heavily

rely on adjusting band structure parameters, like the next nearest neighbor hopping t', *etc.* To the best of our knowledge, the ICAF and commensurate resonance peak in underdoped bilayer cuprates have not yet been treated from a unified point of view for the normal state. No explicit predictions on doping and energy dependence of the ICAF peaks have been made so far.

In our earlier work using the fermion-spin theory, [19] the dynamical spin structure factor (DSSF) has been calculated for LSCO within the single layer t-J model [20], and the obtained doping dependence of the IC parameter δ is consistent with experiments. [1–3] In this paper we show explicitly if the bilayer interactions are included, one can reproduce all main features in the normal state observed experimentally on YBCO, [8,9] including the doping dependence of ICAF at low energies and $[\pi,\pi]$ resonance at relatively high energy. The bilayer band splitting in BSCO has been observed in the angle-resolved photoemission spectroscopy in both normal and superconducting states. [18] The convergence of ICAF peaks at lower energies to commensurate resonance peak at higher energy is rather similar to the scenario argued in Ref. [10] for the SC state, and the DSSF we derive from the simple t-J model (without additional terms and adjustable parameters) demonstrates explicitly this convergence.

The t-J model in bilayer structures is expressed as,

$$H = -t\sum_{ai\hat{\eta}\sigma} C^{\dagger}_{ai\sigma}C_{ai+\hat{\eta}\sigma} - t_{\perp}\sum_{i\sigma}(C^{\dagger}_{1i\sigma}C_{2i\sigma} + \text{h.c.}) - \mu\sum_{ai\sigma} C^{\dagger}_{ai\sigma}C_{ai\sigma} + J\sum_{ai\hat{\eta}} \mathbf{S}_{ai}\cdot\mathbf{S}_{ai+\hat{\eta}} + J_{\perp}\sum_{i}\mathbf{S}_{1i}\cdot\mathbf{S}_{2i}, \tag{1}$$

where $\hat{\eta} = \pm\hat{x},\ \pm\hat{y},\ a = 1,2$ is plane indices, and $\mathbf{S}_{ai} = C^{\dagger}_{ai}\vec{\sigma}C_{ai}/2$ are spin operators with $\vec{\sigma} = (\sigma_x,\sigma_y,\sigma_z)$ as Pauli matrices. The t-J Hamiltonian is supplemented by the single occupancy local constraint $\sum_{\sigma} C^{\dagger}_{ai\sigma}C_{ai\sigma} \leq 1$. This local constraint can be treated *properly in analytical form* within the fermion-spin theory [19] based on the slave particle approach,

$$C_{ai\uparrow} = h^{\dagger}_{ai}S^{-}_{ai}, \quad C_{ai\downarrow} = h^{\dagger}_{ai}S^{+}_{ai}, \tag{2}$$

where the spinless fermion operator h_{ai} keeps track of the charge (holon), while the pseu-

dospin operator S_{ai} keeps track of the spin (spinon), and the *low-energy* Hamiltonian of the bilayer t-J model (1) can be rewritten in the fermion-spin representation as,

$$H = t\sum_{ai\hat{\eta}} h^{\dagger}_{ai+\hat{\eta}} h_{ai}(S^{+}_{ai}S^{-}_{ai+\hat{\eta}} + S^{-}_{ai}S^{+}_{ai+\hat{\eta}}) + t_{\perp}\sum_{i}(h^{\dagger}_{1i}h_{2i} + h^{\dagger}_{2i}h_{1i})(S^{+}_{1i}S^{-}_{2i} + S^{-}_{1i}S^{+}_{2i}) + \mu\sum_{ai} h^{\dagger}_{ai}h_{ai} + J_{\rm eff}\sum_{ai\hat{\eta}} \mathbf{S}_{ai}\cdot\mathbf{S}_{ai+\hat{\eta}} + J_{\perp{\rm eff}}\sum_{i}\mathbf{S}_{1i}\cdot\mathbf{S}_{2i}, \tag{3}$$

with $J_{\rm eff} = J[(1-p)^2 - \phi^2]$ and $J_{\perp{\rm eff}} = J[(1-p)^2 - \phi^2_{\perp}]$, where p is the hole doping concentration, the holon in-plane and bilayer hopping parameters $\phi = \langle h^{\dagger}_{ai}h_{ai+\hat{\eta}}\rangle$ and $\phi_{\perp} = \langle h^{\dagger}_{1i}h_{2i}\rangle$, and S^{+}_{ai} (S^{-}_{ai}) as the pseudospin raising (lowering) operators. In the bilayer system, because of the two coupled CuO_2 planes, the energy spectrum has two branches. In this case, the one-particle spinon and holon Green's functions are matrices, and are expressed as,

$$D(i-j,\tau-\tau') = D_L(i-j,\tau-\tau') + \tau_x D_T(i-j,\tau-\tau'),$$
$$g(i-j,\tau-\tau') = g_L(i-j,\tau-\tau') + \tau_x g_T(i-j,\tau-\tau'), \tag{4}$$

respectively, where the longitudinal and transverse parts are defined as,

$$D_L(i-j,\tau-\tau') = -\langle T_{\tau}S^{+}_{ai}(\tau)S^{-}_{aj}(\tau')\rangle,$$
$$g_L(i-j,\tau-\tau') = -\langle T_{\tau}h_{ai}(\tau)h^{\dagger}_{aj}(\tau')\rangle,$$
$$D_T(i-j,\tau-\tau') = -\langle T_{\tau}S^{+}_{ai}(\tau)S^{-}_{a'j}(\tau')\rangle,$$
$$g_T(i-j,\tau-\tau') = -\langle T_{\tau}h_{ai}(\tau)h^{\dagger}_{a'j}(\tau')\rangle, \tag{5}$$

with $a \neq a'$, while τ_x is the Pauli matrix in the pseudospin space of the layer index. Within this framework, the spin fluctuations only couple to spinons, but the strong correlation between holons and spinons is included self-consistently through the holon's parameters entering the spinon propagator. Therefore both spinons and holons are involved in the spin dynamics. The universal behavior of the integrated spin response and ICAF in underdoped single layer cuprates have been discussed within the fermion-spin theory by considering spinon fluctuations around the mean-field (MF) solution, [20] where the spinon part is treated

by the loop expansion to the second order. Following the previous discussions for the single layer case, DSSF of bilayer cuprates is obtained explicitly as,

$$\begin{aligned} S(\mathbf{k},\omega) &= -2[1+n_B(\omega)][2\mathrm{Im}D_L(\mathbf{k},\omega)+2\mathrm{Im}D_T(\mathbf{k},\omega)] \\ &= -\frac{4[1+n_B(\omega)](B_k^{(1)})^2\mathrm{Im}\Sigma_{LT}^{(s)}(\mathbf{k},\omega)}{[\omega^2-(\omega_k^{(1)})^2-B_k^{(1)}\mathrm{Re}\Sigma_{LT}^{(s)}(\mathbf{k},\omega)]^2+[B_k^{(1)}\mathrm{Im}\Sigma_{LT}^{(s)}(\mathbf{k},\omega)]^2}, \end{aligned} \tag{6}$$

where the full spinon Green's function,

$$D^{-1}(\mathbf{k},\omega) = D^{(0)-1}(\mathbf{k},\omega) - \Sigma^{(s)}(\mathbf{k},\omega), \tag{7}$$

with the longitudinal and transverse MF spinon Green's functions,

$$\begin{aligned} D_L^{(0)}(\mathbf{k},\omega) &= 1/2\sum_\nu B_k^{(\nu)}/[\omega^2-(\omega_k^{(\nu)})^2], \\ D_T^{(0)}(\mathbf{k},\omega) &= 1/2\sum_\nu (-1)^{\nu+1}B_k^{(\nu)}/[\omega^2-(\omega_k^{(\nu)})^2], \end{aligned} \tag{8}$$

respectively, where $\nu = 1, 2$, and

$$\begin{aligned} \mathrm{Im}\Sigma_{LT}^{(s)}(\mathbf{k},\omega) &= \mathrm{Im}\Sigma_L^{(s)}(\mathbf{k},\omega)+\mathrm{Im}\Sigma_T^{(s)}(\mathbf{k},\omega), \\ \mathrm{Re}\Sigma_{LT}^{(s)}(\mathbf{k},\omega) &= \mathrm{Re}\Sigma_L^{(s)}(\mathbf{k},\omega)+\mathrm{Re}\Sigma_T^{(s)}(\mathbf{k},\omega), \end{aligned} \tag{9}$$

while $\mathrm{Im}\Sigma_L^{(s)}(\mathbf{k},\omega)$ ($\mathrm{Im}\Sigma_T^{(s)}(\mathbf{k},\omega)$) and $\mathrm{Re}\Sigma_L^{(s)}(\mathbf{k},\omega)$ ($\mathrm{Re}\Sigma_T^{(s)}(\mathbf{k},\omega)$) are the imaginary and real parts of the second order longitudinal (transverse) spinon self-energy, respectively, obtained from the holon bubble as,

$$\begin{aligned} \Sigma_L^{(s)}(\mathbf{k},\omega) &= (1/N)^2\sum_{pp'}\sum_{\nu\nu'\nu''}\Pi_{\nu\nu'\nu''}(\mathbf{k},\mathbf{p},\mathbf{p}',\omega), \\ \Sigma_T^{(s)}(\mathbf{k},\omega) &= (1/N)^2\sum_{pp'}\sum_{\nu\nu'\nu''}(-1)^{\nu+\nu'+\nu''+1}\Pi_{\nu\nu'\nu''}(\mathbf{k},\mathbf{p},\mathbf{p}',\omega), \end{aligned} \tag{10}$$

with

$$\begin{aligned} \Pi_{\nu\nu'\nu''}(\mathbf{k},\mathbf{p},\mathbf{p}',\omega) &= \left(Zt[\gamma_{p'+p+k}+\gamma_{k-p'}]+t_\perp[(-1)^{\nu'+\nu''}+(-1)^{\nu+\nu''}]\right)^2\frac{B_{k+p}^{(\nu'')}}{16\omega_{k+p}^{(\nu'')}} \\ &\times\left(\frac{F_{\nu\nu'\nu''}^{(1)}(\mathbf{k},\mathbf{p},\mathbf{p}')}{\omega+\xi_{p+p'}^{(\nu')}-\xi_{p'}^{(\nu)}-\omega_{k+p}^{(\nu'')}}-\frac{F_{\nu\nu'\nu''}^{(2)}(\mathbf{k},\mathbf{p},\mathbf{p}')}{\omega+\xi_{p+p'}^{(\nu')}-\xi_{p'}^{\nu}+\omega_{k+p}^{(\nu'')}}\right), \end{aligned} \tag{11}$$

where $\gamma_{\mathbf{k}} = (1/Z)\sum_{\hat{\eta}} e^{i\mathbf{k}\cdot\hat{\eta}}$, Z is the coordination number,

$$B_k^{(\nu)} = B_k - J_{\perp\mathrm{eff}}[\chi_\perp + 2\chi_\perp^z(-1)^\nu][\epsilon_\perp + (-1)^\nu]$$

$$B_k = \lambda[(2\epsilon\chi^z + \chi)\gamma_k - (\epsilon\chi + 2\chi^z)], \quad \lambda = 2ZJ_{\mathrm{eff}},$$

$$\epsilon = 1 + 2t\phi/J_{\mathrm{eff}}, \quad \epsilon_\perp = 1 + 4t_\perp\phi_\perp/J_{\perp\mathrm{eff}},$$

$$F^{(1)}_{\nu\nu'\nu''}(\mathbf{k},\mathbf{p},\mathbf{p}') = n_F(\xi^{(\nu')}_{p+p'})[1 - n_F(\xi^{(\nu)}_{p'})] - n_B(\omega^{(\nu'')}_{k+p})[n_F(\xi^{(\nu)}_{p'}) - n_F(\xi^{(\nu')}_{p+p'})],$$

$$F^{(2)}_{\nu\nu'\nu''}(\mathbf{k},\mathbf{p},\mathbf{p}') = n_F(\xi^{(\nu')}_{p+p'})[1 - n_F(\xi^{(\nu)}_{p'})] + [1 + n_B(\omega^{(\nu'')}_{k+p})][n_F(\xi^{(\nu)}_{p'}) - n_F(\xi^{(\nu')}_{p+p'})], \tag{12}$$

$n_F(\xi_k^{(\nu)})$ and $n_B(\omega_k^{(\nu)})$ are the fermion and boson distribution functions, respectively, and the MF holon and spinon excitations,

$$\xi_k^{(\nu)} = 2Zt\chi\gamma_k + \mu + 2\chi_\perp t_\perp(-1)^{\nu+1},$$
$$(\omega_k^{(\nu)})^2 = \omega_k^2 + \Delta_k^2(-1)^{\nu+1}, \tag{13}$$

with $\omega_k^2 = A_1\gamma_k^2 + A_2\gamma_k + A_3$, $\Delta_k^2 = X_1\gamma_k + X_2$,

$$A_1 = \alpha\epsilon\lambda^2(\chi/2 + \epsilon\chi^z),$$

$$A_2 = \epsilon\lambda^2[(1-Z)\alpha(\epsilon\chi/2 + \chi^z)/Z - \alpha(C^z + C/2) - (1-\alpha)/(2Z)]$$
$$-\alpha\lambda J_{\perp\mathrm{eff}}[\epsilon(C_\perp^z + \chi_\perp^z) + \epsilon_\perp(C_\perp + \epsilon\chi_\perp)/2],$$

$$A_3 = \lambda^2[\alpha(C^z + \epsilon^2 C/2) + (1-\alpha)(1+\epsilon^2)/(4Z) - \alpha\epsilon(\chi/2 + \epsilon\chi^z)/Z]$$
$$+\alpha\lambda J_{\perp\mathrm{eff}}[\epsilon\epsilon_\perp C_\perp + 2C_\perp^z] + J^2_{\perp\mathrm{eff}}(\epsilon_\perp^2 + 1)/4,$$

$$X_1 = \alpha\lambda J_{\perp\mathrm{eff}}[(\epsilon_\perp\chi + \epsilon\chi_\perp)/2 + \epsilon\epsilon_\perp(\chi_\perp^z + \chi^z)],$$

$$X_2 = -\alpha\lambda J_{\perp\mathrm{eff}}[\epsilon\epsilon_\perp\chi/2 + \epsilon_\perp(\chi^z + C_\perp^z) + \epsilon C_\perp/2] - \epsilon_\perp J^2_{\perp\mathrm{eff}}/2, \tag{14}$$

the spinon correlation functions $\chi = \langle S^+_{ai}S^-_{ai+\hat{\eta}}\rangle$, $\chi^z = \langle S^z_{ai}S^z_{ai+\hat{\eta}}\rangle$, $\chi_\perp = \langle S^+_{1i}S^-_{2i}\rangle$, $\chi_\perp^z = \langle S^z_{1i}S^z_{2i}\rangle$, $C = (1/Z^2)\sum_{\hat{\eta}\hat{\eta}'}\langle S^+_{ai+\hat{\eta}}S^-_{ai+\hat{\eta}'}\rangle$, and $C^z = (1/Z^2)\sum_{\hat{\eta}\hat{\eta}'}\langle S^z_{ai+\hat{\eta}}S^z_{ai+\hat{\eta}'}\rangle$, $C_\perp = (1/Z)\sum_{\hat{\eta}}\langle S^+_{2i}S^-_{1i+\hat{\eta}}\rangle$, and $C_\perp^z = (1/Z)\sum_{\hat{\eta}}\langle S^z_{1i}S^z_{2i+\hat{\eta}}\rangle$. In order to satisfy the sum rule for the correlation function $\langle S^+_{ai}S^-_{ai}\rangle = 1/2$ in the absence of AF long range order (AFLRO), a decoupling parameter α has been introduced in the MF calculation, which can be regarded as the vertex correction. [21] All these parameters have been determined self-consistently, as done in the single layer case. [20]

At half-filling, the t-J model is reduced to the Heisenberg AF model, and the AFLRO gives rise to a commensurate peak at $[1/2, 1/2]$ (hereafter we use the units of $[2\pi, 2\pi]$). In Fig. 1, we plot DSSF $S(\mathbf{k}, \omega)$ in the (k_x, k_y) plane at doping $p = 0.06$, temperature $T = 0.1J$ and energy $\omega = 0.35J$ for $t/J = 2.5$, $t_\perp/t = 0.25$, and $J_\perp/J = 0.25$, which shows that a commensurate-IC transition in the spin fluctuation pattern occurs with doping. At low energies and lower temperatures, the commensurate peak close to half-filling is split into four peaks at $[(1 \pm \delta)/2, 1/2]$ and $[1/2, (1 \pm \delta)/2]$. The calculated DSSF $S(\mathbf{k}, \omega)$ has been used to extract the doping dependence of the IC parameter $\delta(p)$, defined as the deviation of the peak position from the AF wave vector $[1/2, 1/2]$, and the result is shown in Fig. 2 in comparison with the experimental data [9] taken on YBCO (inset). $\delta(p)$ increases initially with the hole concentration in the low doping regime, but it saturates quickly at higher dopings, in semi-quantitative agreement with the experimental data. [9] Apparently, there is a substantial difference between theory and experiment, namely the saturation occurs at $p = 0.10$ in experiment, while the calculation anticipates it already at $p \approx 0.05$. However, upon a closer examination one sees immediately that the main difference is due to the appearance of ICAF at too low dopings in the theoretical consideration. The actual range of rapid growth of IC parameter $\delta(p)$ with doping p (around $4 \sim 5\%$) is very similar in theory and experiment.

For considering the resonance at relatively high energy we have made a series of scans for $S(\mathbf{k}, \omega)$ at different energies, and the result for doping $p = 0.06$, $t/J = 2.5$, $t_\perp/t = 0.25$, $J_\perp/J = 0.25$ at $T = 0.1J$ and $\omega = 0.5J$ is shown in Fig. 3. Comparing it with Fig. 1 for the same set of parameters except for $\omega = 0.35J$, we see that IC peaks are energy dependent, *i.e.*, although these magnetic scattering peaks retain the IC pattern at $[(1 \pm \delta)/2, 1/2]$ and $[1/2, (1 \pm \delta)/2]$ in low energies, the positions of IC peaks move towards $[1/2, 1/2]$ with increasing energy, and then the $[1/2, 1/2]$ resonance peak appears at relatively high energy ($\omega_r = 0.5J$). To show this point clearly, we plot the evolution of the magnetic scattering peaks with energy in Fig. 4. For comparison, the experimental result [10] of $YBa_2Cu_3O_{6+x}$ with $x = 0.85$ ($p \approx 0.14$) for the SC state is shown in the same figure. A similar experimental

result [8] has also been obtained for $YBa_2Cu_3O_{6+x}$ with $x = 0.7$ ($p \approx 0.12$). Although these experimental data were obtained below T_c, they also hold for the normal state in the underdoped regime $x \leq 0.7$ ($p \leq 0.12$). [9] The anticipated position $\omega_r = 0.5J \approx 50$ mev [22] is not too far from the peak $\approx$ 30mev $\sim$ 37mev observed in underdoped YBCO. [9] Moreover, the resonance energy ω_r is proportional to p at small dopings. We have also made a series of scans for $S(\mathbf{k}, \omega)$ at different temperatures, and found both IC peaks and resonance peak are broadened and suppressed with increasing temperature, and tend to vanish at high temperatures. This reflects that the spin excitations are rather sharp in momentum space at low temperatures, compared with the linewidth, and the inverse lifetime increases with increasing temperature. Our result is in qualitative agreement with experiments. [9]

Now we turn to discuss the integrated spin response, which is manifested by the integrated dynamical spin susceptibility, and can be expressed as,

$$I(\omega, T) = (1/N) \sum_k \chi''(\mathbf{k}, \omega), \tag{15}$$

where the dynamical spin susceptibility is related to DSSF by the fluctuation-dissipation theorem as, $\chi''(\mathbf{k}, \omega) = (1 - e^{-\beta\omega}) S(\mathbf{k}, \omega)$. The results of $I(\omega, T)$ at doping $p = 0.06$ in $t/J = 2.5$, $t_\perp/t = 0.25$, and $J_\perp/J = 0.25$ with $T = 0.1J$ (solid line) and $T = 0.2J$ (dashed line) are plotted in Fig. 5 in comparison with the experimental data [23] taken from $YBa_2Cu_3O_{6+x}$ (inset), where the dotted line is the function $\sim \arctan[a_1\omega/T + a_3(\omega/T)^3]$ with $a_1 = 6.6$, and $a_3 = 3.9$. These results show that $I(\omega, T)$ is almost constant for $\omega/T > 1$ and then begin to decrease with decreasing ω/T for $\omega/T < 1$. It is quite remarkable that the integrated susceptibility in the bilayer cuprates shows the same universal behavior as in the case of the single layer cuprates, [20] and is scaled approximately as $I(\omega, T) \propto \arctan[a_1\omega/T + a_3(\omega/T)^3]$. This result is consistent with experiments. [23]

The DSSF in Eq. (3) has a well-defined resonance character, where $S(\mathbf{k}, \omega)$ exhibits peaks when the incoming neutron energy ω is equal to the renormalized spin excitation $E_k^2 = (\omega_k^{(1)})^2 + B_k^{(1)} \mathrm{Re}\Sigma_{LT}^{(s)}(\mathbf{k}, E_k)$, *i.e.*, $W(\mathbf{k}_c, \omega) \equiv [\omega^2 - (\omega_{k_c}^{(1)})^2 - B_{k_c}^{(1)} \mathrm{Re}\Sigma_{LT}^{(s)}(\mathbf{k}_c, \omega)]^2 = (\omega^2 - E_{k_c}^2)^2 \sim 0$ for certain critical wave vectors $\mathbf{k}_c$. The height of these peaks is determined

by the imaginary part of the spinon self-energy $1/\mathrm{Im}\Sigma^{(s)}_{LT}(\mathbf{k}_c,\omega)$. This renormalized spin excitation is doping and energy dependent. Since $\mathrm{Re}\Sigma^{(s)}_{LT}(\mathbf{k},\omega)=\mathrm{Re}\Sigma^{(s)}_{L}(\mathbf{k},\omega)+\mathrm{Re}\Sigma^{(s)}_{T}(\mathbf{k},\omega)$ with $\mathrm{Re}\Sigma^{(s)}_{L}(\mathbf{k},\omega)<0$ and $\mathrm{Re}\Sigma^{(s)}_{T}(\mathbf{k},\omega)>0$, there is a competition between $\mathrm{Re}\Sigma^{(s)}_{L}(\mathbf{k},\omega)$ and $\mathrm{Re}\Sigma^{(s)}_{T}(\mathbf{k},\omega)$, which comes entirely from the bilayer band splitting. [18] At low energies the main contribution to $\mathrm{Re}\Sigma^{(s)}_{LT}(\mathbf{k},\omega)$ comes from $\mathrm{Re}\Sigma^{(s)}_{L}(\mathbf{k},\omega)$, then ICAF emerges, where the essential physics is almost the same as in single layer cuprates, and detailed explanations have been given in Ref. [20]. Near half-filling, the spin excitations are centered around the AF wave vector [1/2, 1/2], so the commensurate AF peak appears there. Upon doping, the holes disturb the AF background. Within the fermion-spin framework, as a result of self-consistent motion of holons and spinons, ICAF is developed beyond certain critical doping, which means, the low-energy spin excitations drift away from the AF wave vector, or the zero of $W(\mathbf{k}_\delta,\omega)$ is shifted from $[1/2,1/2]$ to $\mathbf{k}_\delta$, where the physics is dominated by the spinon self-energy $\mathrm{Re}\Sigma^{(s)}_{L}(\mathbf{k},\omega)$ renormalization due to holons. In this sense, the mobile holes are the key factor leading to ICAF. However, $\mathrm{Re}\Sigma^{(s)}_{T}(\mathbf{k},\omega)$ cancels out most contributions from $\mathrm{Re}\Sigma^{(s)}_{L}(\mathbf{k},\omega)$ at relatively high energy, then the anomalous $[1/2,1/2]$ resonance reappears. Therefore the bilayer band splitting plays a crucial role in giving rise to the resonance. What we calculate is the acoustic spin excitation with modulations in the c-direction $\propto \sin^2(\pi z_{Cu}L)$, where z_{Cu} is the distance between two nearest Cu layers, L the c-axis coordinate in the reciprocal space. This reflects the *antiferromagnetic coupling* between layers, and it is fully confirmed by experiments. [8–10]

In conclusion we have shown that if the strong spinon-holon interaction and bilayer interactions are taken into account, the t-J model per se can correctly reproduce all main features of INS experiments in the *normal state* in underdoped bilayer cuprates, including the doping and energy dependence of ICAF at low energies and $[1/2,1/2]$ resonance at relatively high energy. In fact the ICAF peaks converge to the commensurate resonance, as the energy is increased. In our opinion, the difference of AF fluctuation behavior between LSCO and YBCO (BSCO) is not due to the presence/absence of stripes, but rather because of the

single/double layer structure. Of course, this has to be checked by further experiments. It is possible that at some particular energy, a strong commensurate resonance peak coexists with the weaker IC features as shown in Fig. 3.

After submitting this paper, we became aware of the recent INS measurements [24] providing evidence for a sharp commensurate resonance peak below T_c in the single layer cuprate $Tl_2Ba_2Cu_{6+\delta}$ near optimal doping. However, above T_c, the experimental scans show a featureless background that gradually decreases in an energy- and momentum-independent fashion as the temperature is lowered. The INS in the SC state has not been considered so far within the fermion-spin approach, and we need to extend our studies for both single layer [20] and bilayer cases to the SC state, where the holon Cooper pairs are formed, and the spinon self-energy is originating from both normal and *anomalous* holon bubbles. Hence the renormalized spin excitation in the SC state is very much different from that in the *normal state*, and it may be related to the magnetic peaks detected in the SC state. These and other related issues are under investigation now. On the other hand, we emphasize that although the simple t-J model can not be regarded as a comprehensive model for the quantitative comparison with the doped cuprates, our present results for the *normal state* are in semi-quantitative agreement with the major experimental observations in the *normal state* of the underdoped bilayer cuprates. [9,10,23].

ACKNOWLEDGMENTS

This work was supported by the National Natural Science Foundation of China under Grant Nos. 10074007, 10125415, and 90103024.

REFERENCES

[1] For reviews, see M.A.Kastner, R.J. Birgeneau, G. Shiran, Y. Endoh, Rev. Mod. Phys. **70**, 897 (1998); A.P. Kampf, Phys. Rep. **249**, 219 (1994).

[2] K. Yamada, C.H. Lee, K. Kurahashi, J. Wada, S. Wakimoto, S. Ueki, H. Kimura, Y. Endoh, S. Hosoya, and G. Shirane, Phys. Rev. B **57**, 6165 (1998), and references therein.

[3] G. Aeppli, T.E. Mason, S.M. Hayden, H.A. Mook, and J. Kulda, Science **278**, 1432 (1997).

[4] J. Rossat-Mignod, L.P. Regnault, P. Bourges, P. Burlet, J. Bossy, J.Y. Henri, and G. Lapertot, Physica C **185-189**, 86 (1991).

[5] H.A. Mook, M. Yethiraj, G. Aeppli, T.E. Mason, and T. Armstrong, Phys. Rev. Lett. **70**, 3490 (1993); H.F. Fong, B. Keimer, P.W. Anderson, D. Reznik, F. Doğan, and I.A. Aksay, Phys. Rev. Lett. **75**, 316 (1995); P. Bourges, L.P. Regnault, Y. Sidis, and C. Vettier, Phys. Rev. B **53**, 876 (1996).

[6] P. Dai, M. Yethiraj, H.A. Mook, T.B. Lindemer, and F. Doğan, Phys. Rev. Lett. **77**, 5425 (1996); H.F. Fong, B. Keimer, F. Doğan, and I.A. Aksay, Phys. Rev. Lett. **78**, 713 (1997); P. Bourges, L.P. Regnault, Y. Sidis, J. Bossy, P. Burlet, C. Vettier, J.Y. Henry, and M. Couach, Europhys. Lett. **38**, 313 (1997).

[7] H.F. Fong, P. Bourges, Y. Sidis, L.P. Regnault, A. Ivanov, G.D. Gu, N. Koshizuka, and B. Keimer, Nature **398**, 588 (1999); H. He, Y. Sidis, P. Bourges, G.D. Gu, A. Ivanov, N. Koshizuka, B. Liang, C.T. Lin, L.P. Regnault, E. Schoenherr, and B. Keimer, Phys. Rev. Lett. **86**, 1610 (2001).

[8] H.A. Mook, P. Dai, S.M. Hayden, G. Aeppli, T.J. Perring, and F. Doğan, Nature **395**, 580 (1998); M. Arai, T. Nishijima, Y. Endoh, T. Egami, S. Tajima, K. Tomimoto, Y. Shiohara, M. Takahashi, A. Garret, and S.M. Bennington, Phys. Rev. Lett. **83**, 608 (1999); P. Dai, H.A. Mook, S.M. Hayden, G. Aeppli, T.J. Perring, R.D. Hunt, and F.

Doğan, Science **284**, 1344 (1999).

[9] P. Dai, H.A. Mook, R.D. Hunt, and F. Doğan, Phys. Rev. B**63**, 54525 (2001), and references therein.

[10] P. Bourges, Y. Sidis, H.F. Fong, L.P. Regnault, J. Bossy, A. Ivanov, and B. Keimer, Science **288**, 1234 (2000); P. Bourges, B. Keimer, L.P. Regnault, and Y. Sidis, cond-mat/0006085.

[11] See, *e.g.*, N. Bulut, D. Hone, D.J. Scalapino, and N.E. Bickers, Phys. Rev. Lett **64**, 2723 (1990); Q. Si, Y. Zha, K. Levin, and J.P. Lu, Phys. Rev. B **47**, 9055 (1993); T. Tanamoto, H. Kohno, and H. Fukuyama, J. Phys. Soc. Jpn. **63**, 2739 (1994).

[12] See, *e.g.*, G. Blumberg, B.P. Stojkovic, and M.V. Klein, Phys. Rev. B **52**, 15741 (1995); D.Z. Liu, Y. Zha, and K. Levin, Phys. Rev. Lett. **75**, 4130 (1995) and more references in Ref. [15].

[13] See, *e.g.*, J. Zaanen and O. Gunnarsson, Phys. Rev. B **40**, 7391 (1989); D. Poilblanc and T.M. Rice, Phys. Rev. B **39**, 9749 (1989).

[14] D.K. Morr and D. Pines, Phys. Rev. Lett. **81**, 1086 (1998); F. Onufrieva and P. Pfeuty, cond-mat/9903097; A. Abanov and A.V. Chubukov, Phys. Rev. Lett. **83**, 1652 (1999). J.Y. Kao, Q. Si, and K. Levin,, Phys. Rev. B **61**, 11898 (2000); M.R. Norman, Phys. Rev. B **61**, 14751 (2000).

[15] J. Brinckmann and P.A. Lee, Phys. Rev. Lett. **82**, 2915 (1999); *ibid*, cond-mat/0107138.

[16] E. Demler and S.C. Zhang, Phys. Rev. Lett. **75**, 4126 (1995); E. Demler, H. Kohno, and S.C. Zhang, Phys. Rev. B **58**, 5719 (1998).

[17] L. Yin, S. Chakravarty, and P.W. Anderson, Phys. Rev. Lett. **78**, 3559 (1997).

[18] D.L. Feng, N.P. Armitage, D.H. Lu, A. Damascelli, J.P. Hu, P. Bogdanov, A. Lanzara, F. Ronning, K.M. Shen, H. Eisaki, C. Kim, Z.X. Shen, J.-i. Shimoyama, and K. Kishio,

Phys. Rev. Lett. **86**, 5550 (2001).

[19] Shiping Feng, Z.B. Su, and L. Yu, Phys. Rev. B **49**, 2368 (1994); Mod. Phys. Lett. B**7**, 1013 (1993).

[20] Feng Yuan, Shiping Feng, Zhao-Bin Su, and Lu Yu, Phys. Rev. B **64**, 224505 (2001); Shiping Feng and Zhongbing Huang, Phys. Rev. B **57**, 10328 (1998).

[21] Shiping Feng and Yun Song, Phys. Rev. B **55**, 642 (1997); J. Kondo and K. Yamaji, Prog. Theor. Phys. **47**, 807 (1972).

[22] S. Shamoto, M. Sato, J.M. Tranquada, B.J. Sternlib, and G. Shirane, Phys. Rev. B **48**, 13817 (1993).

[23] R.J. Birgeneau, R.W. Erwin, P.G. Gehring, B. Keimer, M.A. Kastner, M. Sato, S. Shamoto, G. Shirane, and J.M. Tranquada, Z. Phys. B**87**, 15 (1992); B.J. Sternlieb, G. Shirane, J.M. Tranquada, M. Sato, and S. Shamoto, Phys. Rev. B **47**, 5320 (1993).

[24] H. He, P. Bourges, Y. Sidis, C. Ulrich, L.P. Regnault, S. Pailhés, N.S. Berzigiarova, N.N. Kolesnikov, and B. Keimer, Science **295**, 1045 (2002).

FIGURES

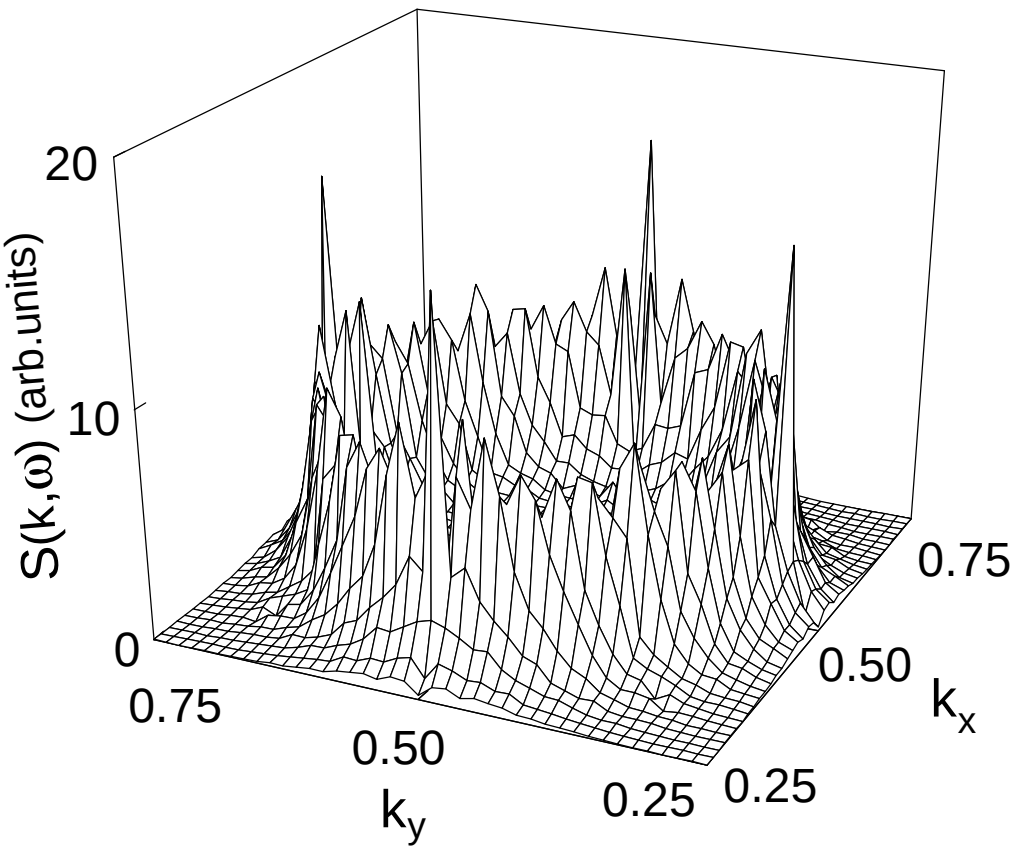
FIG. 1. The dynamical spin structure factor in the (k_x, k_y) plane at doping $p = 0.06$, temperature $T = 0.1J$ and energy $\omega = 0.35J$ for $t/J = 2.5$, $t_\perp/t = 0.25$, and $J_\perp/J = 0.25$. A quasiparticle damping $\Gamma = 0.01J$ has been used in all results presented.

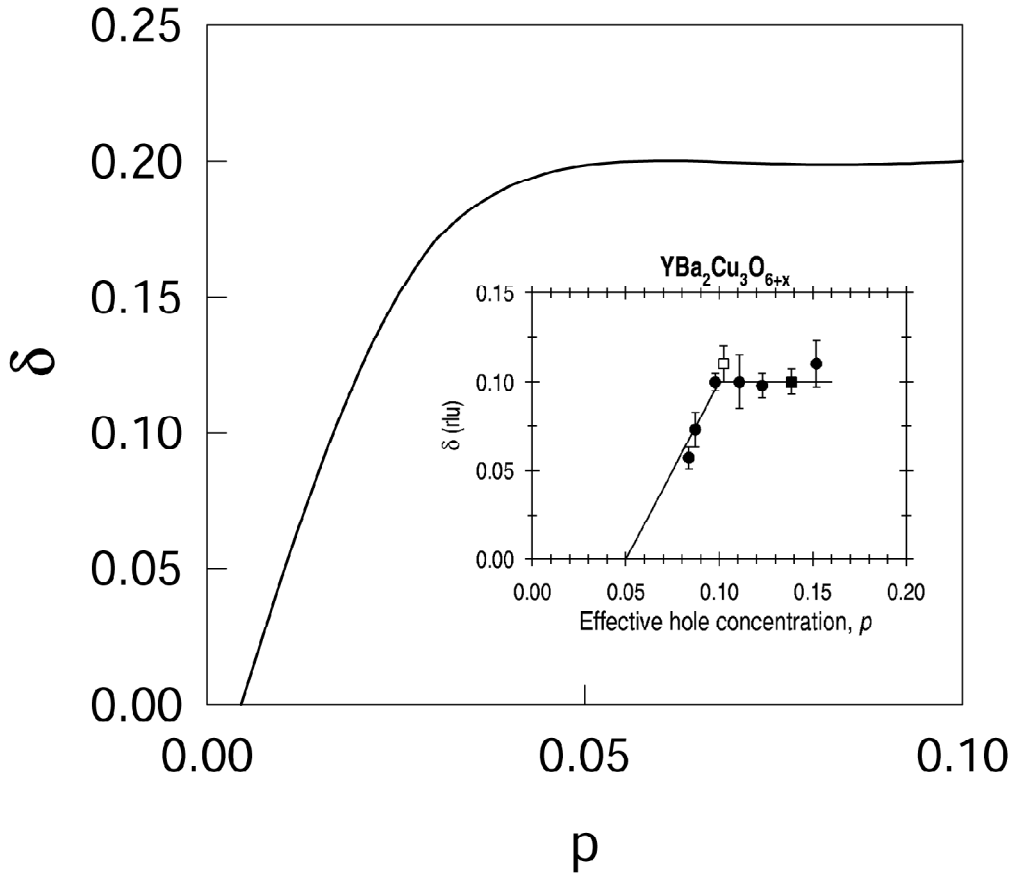
FIG. 2. The doping dependence of the incommensurability $\delta(p)$ of the antiferromagnetic fluctuations. Inset: the experimental results on YBCO taken from Ref. [9].

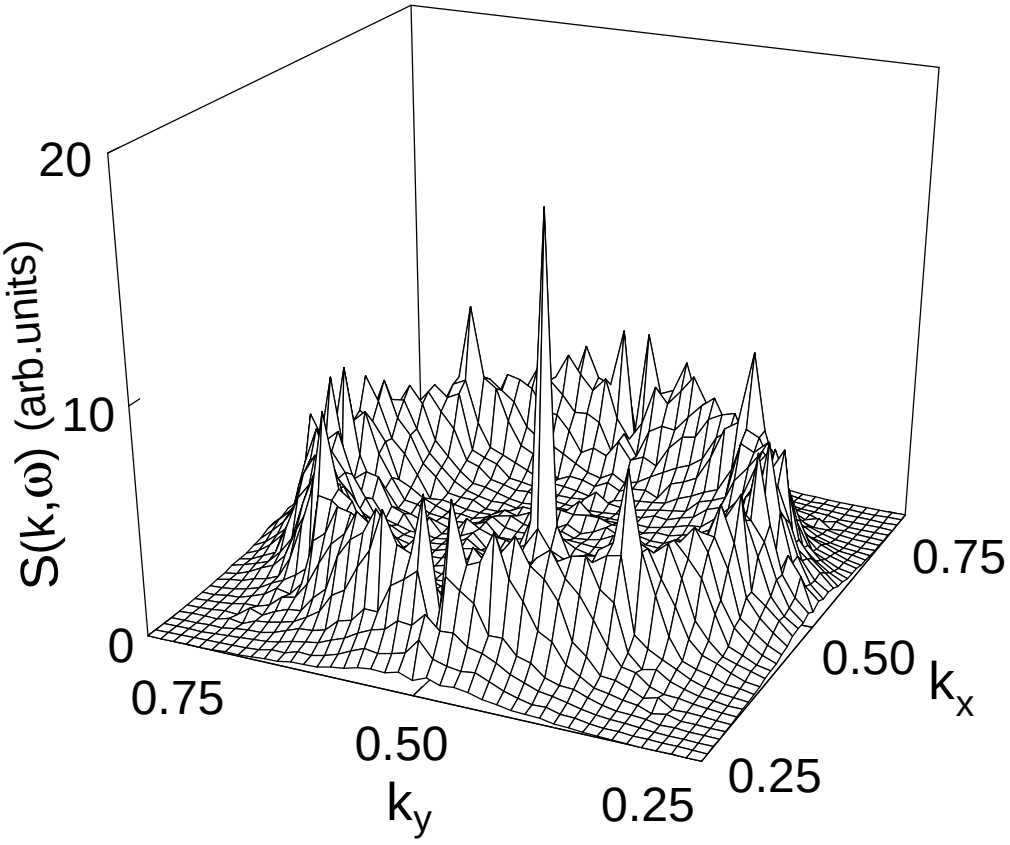
FIG. 3. The dynamical spin structure factor in the (k_x, k_y) plane at $p = 0.06$ for $t/J = 2.5$, $t_\perp/t = 0.25$, $J_\perp/J = 0.25$ and $\omega = 0.5J$ at $T = 0.1J$.

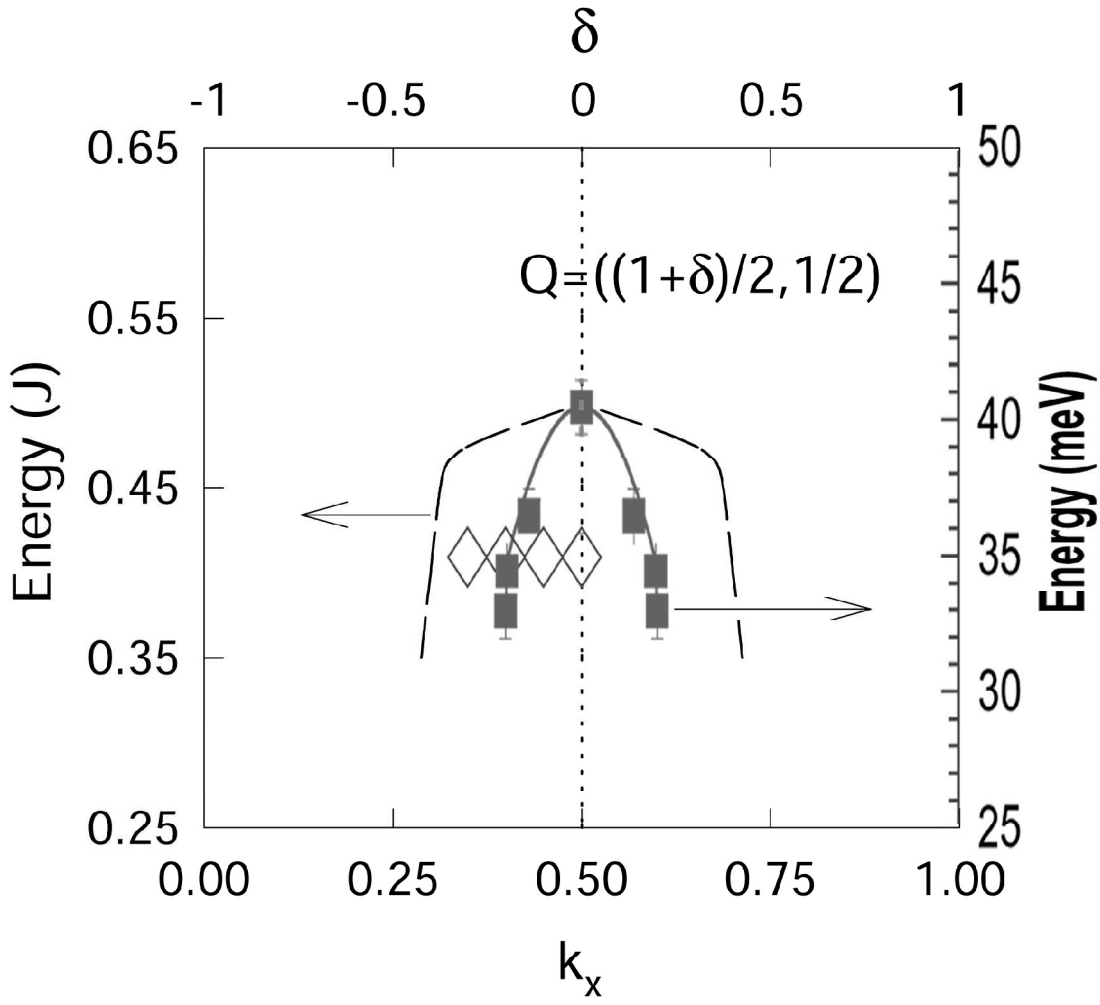
FIG. 4. The energy dependence of the position of the incommensurate peaks at $p = 0.06$ and $T = 0.1J$ for $t/J = 2.5$, $t_\perp/t = 0.25$, and $J_\perp/J = 0.25$ (left ordinates) vs the experimental results on $YBa_2Cu_3O_{6.85}$ in the superconducting state taken from Ref. [10] (right ordinates).

FIG. 5. The integrated susceptibility at $p = 0.06$ for $t/J = 2.5$, $t_\perp/t = 0.25$, and $J_\perp/J = 0.25$ in $T = 0.1J$ (solid line) and $T = 0.2J$ (dashed line). The dotted line is the function $b_1 \arctan[a_1\omega/T + a_3(\omega/T)^3]$ with $a_1 = 6.6$ and $a_3 = 3.9$. Inset: the experimental result on $YBa_2Cu_3O_{7-x}$ taken from Ref. [23].


20
10
0
S(k,ω) (arb.units)
0.75
0.50
0.25
k_y
0.25
0.50
0.75
k_x


0.25
0.20
0.15
0.10
0.05
0.00
δ
0.00
0.05
0.10
p
YBa2Cu3O6+x
0.15
0.10
0.05
0.00
δ (rlu)
0.00
0.05
0.10
0.15
0.20
Effective hole concentration, p


20
10
0
S(k,ω) (arb.units)
0.75
0.50
k_y
0.25
0.75
0.50
k_x
0.25


δ
-1
-0.5
0
0.5
1
Q=((1+δ)/2,1/2)
Energy (J)
0.65
0.55
0.45
0.35
0.25
Energy (meV)
50
45
40
35
30
25
0.00
0.25
0.50
0.75
1.00
k_x